Energy Conversion and Management 50 (2009) 600–610

Contents lists available at ScienceDirect

Energy Conversion and Management

journal homepage: www.elsevier.com/locate/enconman

Complete wind farm electromagnetic transient modelling for grid integration studies

I. Zubia [a,*], X. Ostolaza [b], A. Susperregui [b], G. Tapia [b]

[a] Electrical Engineering Department, University of the Basque Country, Plaza Europa 1, 20018 Donostia-San Sebastián, Spain
[b] Systems Engineering and Control Department, University of the Basque Country, Plaza Europa 1, 20018 Donostia-San Sebastián, Spain

ARTICLE INFO

Article history:
Received 15 June 2007
Received in revised form 2 April 2008
Accepted 28 October 2008
Available online 25 December 2008

Keywords:
Wind power generation
Power system modelling
Rotating machine transient analysis
Multi-machine models
Power system transients
Islanding operation

ABSTRACT

This paper presents a modelling methodology to analyse the impact of wind farms in surrounding networks. Based on the transient modelling of the asynchronous generator, the multi-machine model of a wind farm composed of *N* generators is developed. The model incorporates step-up power transformers, distribution lines and surrounding loads up to their connection to the power network.

This model allows the simulation of symmetric and asymmetric short-circuits located in the distribution network and the analysis of transient stability of wind farms. It can be also used to study the islanding operation of wind farms.

1. Introduction

Distributed energy generation is becoming a larger part of the total generation of power systems worldwide and, in particular, wind energy represents 50% of the total renewable energy in Europe. Aggregate wind power installed in the European Union (EU-27) at the end of 2007 was 56,535 MW, that covers 3.78% of EU-27 electricity consumption [1]. In Spain installed wind power was 15,145 MW, being the second country in the world.

Wind generation provides several advantages over other power generation systems, such as no cooling water use, no carbon dioxide emissions, proximity of generation to local loads and unloading of transmission lines. It may be asserted, however, that as installed wind power expands, issues related to integration, stability effects and voltage impacts become increasingly important [2].

Due to this fact, several transmission system operators have defined specifications for connecting wind farms to their networks [3–5]. The purpose of the specifications is to ensure the essential properties for power system operation as regards security of supply, reliability and power quality. These specifications include frequency and voltage quality conditions, active and reactive power control ability, stability and protection requirements in the case of faults in the power system, and fault ride through capability.

Regarding transient stability, Eltra specification requires that the interaction between the power system and the wind farm at faults in the power system must be verified by means of simulations, and it is the responsibility of the plant owner to provide the necessary models for these simulations [3].

In this context, it is necessary to develop accurate models of wind farms in order to evaluate their impact and predict the farm's influence on the dynamic behaviour of the electrical system [6–11]. With these dynamical models it could be possible to create difficult to test scenarios, such as balanced and unbalanced short-circuits and loss of mains [12–14]. Furthermore, these models could support the design of new protection systems [15], new control algorithms [16–18] and operational strategies to improve their real time exploitation [19], enhancing their collaboration to the support of the electrical grid.

Given that a mathematical modelling of wind farms is a must for their grid integration, a first question arises immediately: which is the appropriate model to analyse consistently the impact of wind farms to the surrounding electrical network?

Typically, two main wind farm modelling tendencies have been observed in references: the aggregated model and the detailed or multi-machine model. The aggregated approach represents a wind farm by one equivalent machine with re-scaled power capacity [6,7]. This model has been applied to the study of voltage stability of the power system [8] as well as to transient stability [9,11], and it has also been tested for load flow analysis [10,20]. On the other

* Corresponding author. Tel.: +34 943017238; fax: +34 943017131.
E-mail addresses: itziar.zubia@ehu.es (I. Zubia), xabier.ostolaza@ehu.es (X. Ostolaza), ana.susperregui@ehu.es (A. Susperregui), gerardo.tapia@ehu.es (G. Tapia).

0196-8904/$ - see front matter © 2008 Elsevier Ltd. All rights reserved.
doi:10.1016/j.enconman.2008.10.024

hand, it allows, under certain conditions, the analysis of transient stability of large wind farms [12,13,21] and their control [16].

The drawback of aggregated models is that they do not reflect effects due to the real operation point of each wind generator, such as mutual interactions or power oscillations between wind turbines. But it is often claimed that aggregated models are able to reflect worst-case scenarios when electrical disturbances affect the normal operation of the wind farm [22]. However, this has resulted not to be exact because they do not describe the general behaviour of wind farms, except in very particular operating conditions [13,19]. To solve this problem several authors have proposed an intermediate detail level where large wind farms are modelled based on wind turbine groups, e.g., an equivalent wind farm for each turbine row [12].

With regard to detailed models, due to their inherent complexity, it is more difficult to find contributions in the bibliography. Several references suggest that multi-machine models are inappropriate because their simulations are much more demanding computationally and that, essentially, the potential advantages do not pay off the additional modelling effort.

But, despite this stance, just a few authors have developed solutions to the detailed model of large wind farms, from two main ways to set out the problem. The first one is the automatic development of simulation models by means of simulation programs, such as PSCAD/EMTDC or SimPowerSystems, which numerically compute the state-space model of the system. With this approach short term voltage stability of the wind farm when the external network is subjected to short-circuits [14], or when there are wind speed changes [23] is analysed. The second option is to explicitly obtain the overall network model, as for the simulation—assuming a simplified generator model—and short-circuit study in an isolated system [24,25]. Obviously, this second approach provides improved knowledge about the system, and interactions among generators are studied with more detail.

This paper presents a methodology to develop electromagnetic transient simulation models of wind farms, to predict their behaviour under normal operating conditions and also under electrical disturbances. It will be assumed that the wind farm will have a radial shape, that is, several generators connected to a common bus bar and, from this a connection line as far as the Point of common coupling to the electric power system.

Simulation models will be developed from a double point of view. Firstly, development of detailed multi-machine models, where each generator has its own point of operation. And secondly, simplified aggregated or macro-generator modelling. Several simulation results of a spanish wind farm, obtained after the implementation of the models in Simulink, are also presented.

2. Electromagnetic transient modelling of the wind generator

In the general case, the electromagnetic transient model of the generator has six differential non-linear equations called *the general three phase model of the machine*. This model describes the evolution of rotor and stator voltages and currents [26]. But, in this model, all six equations are interdependent due to leakage inductances.

To deal with this problem several transformations have been proposed—Clarke's transformation, Park's transformation—that express the original differential equations in different frames of reference, as shown in Fig. 1, where the cross-section of an induction generator containing stator and rotor windings, is depicted. Using these transformations it is possible to refer stator and rotor variables either in the stationary frame "$D-Q-0$", or in a reference frame that rotates with the rotor at its electrical speed ω_r, "$\alpha-\beta-0$" [27].

When induction generator variables are referred to their natural frames, the stator side is referred to the stationary frame

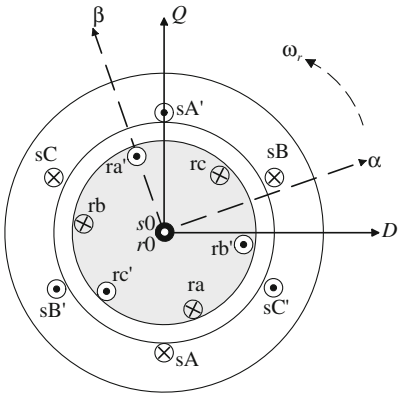

Fig. 1. Schematic cross-section of induction generator.

"$D-Q-0$" and the rotor side is referred to the rotating frame "$\alpha-\beta-0$". This "$sD-sQ-s0-r\alpha-r\beta-r0$" model is also called *"Quadrature-Phase Slip-Ring"* [26].

As Fig. 1 shows, direct and quadrature axes of both frames of reference: stationary—D, Q—and rotating—α, β—are confined in the cross-section of the machine, while zero sequence axis —0—is aligned with the rotor shaft. As a result, zero sequence components are decoupled from direct and quadrature ones, so the original model of six interdependent differential equations leads to a more accessible modelling with just four coupled differential equations plus two independent differential equations.

Furthermore, as zero sequence components cancel out in the case of balanced systems, it is usual to apply only "$D-Q-d-q$" or "$D-Q-\alpha-\beta$" models [16]. Owing to this fact, Clarke's transformation is usually called three to two-axes transformation. However, for a general research about the behaviour of generators under all kind of disturbances (symmetric and asymmetric), this assumption leads to erroneous results, since, in such cases, zero sequence components take non zero values.

In this paper, stator and rotor variables will be expressed in the stationary reference frame "$D-Q-0$", because this modelling approach has three main advantages: firstly electrical parameters of the induction machine are easily calculated from steady-state circuit parameters. Secondly, state equations are much simpler than those of *"Quadrature-Phase Slip-Ring"* model. And finally, calculation of the electromagnetic torque of the generator is straightforward, as we will show below. This model is also known as *"Quadrature-Phase Commutator"* [26].

Keeping in mind all this considerations, the electric model might be expressed through (1)–(6) with currents i_{sD}, i_{sQ}, i_{s0}—for the stator side—i_{rd}, i_{rq}, i_{r0}—for the rotor side—, as electrical state-variables of the electromagnetic transient model. This model will be referred as "$D-Q-0-d-q-0$" [19].

$$\frac{di_{sD}}{dt}=\frac{L_r(v_{sD}-R_s i_{sD})+L_m[\omega_r(L_m i_{sQ}+L_r i_{rq})+R_r i_{rd}-v_{rd}]}{L_m^2-L_s L_r} \tag{1}$$

$$\frac{di_{sQ}}{dt}=\frac{L_r(v_{sQ}-R_s i_{sQ})-L_m[\omega_r(L_m i_{sD}+L_r i_{rd})+R_r i_{rq}+v_{rq}]}{L_m^2-L_s L_r} \tag{2}$$

$$\frac{di_{s0}}{dt}=\frac{-R_s i_{s0}+v_{s0}}{L_{ls}} \tag{3}$$

$$\frac{di_{rd}}{dt}=\frac{L_m(R_s i_{sD}-v_{sD})-L_s[\omega_r(L_m i_{sQ}+L_r i_{rq})+R_r i_{rd}-v_{rd}]}{L_m^2-L_s L_r} \tag{4}$$

$$\frac{di_{rq}}{dt}=\frac{L_m(R_s i_{sQ}-v_{sQ})+L_s[\omega_r(L_m i_{sD}+L_r i_{rd})+R_r i_{rq}+v_{rq}]}{L_m^2-L_s L_r} \tag{5}$$

$$\frac{di_{r0}}{dt}=\frac{-R_r i_{r0}+v_{r0}}{L_{lr}} \tag{6}$$

where L_s and L_r are the stator and rotor side inductances, L_m is the magnetizing inductance, R_s and R_r are the stator and rotor resistances, and ω_r is the rotor electrical speed.

2.1. Mechanical model

The equation that describes the mechanical dynamics of the rotor is

$$T_e + T_w = J\frac{d\omega_{rm}}{dt} + D\omega_{rm} \tag{7}$$

where T_e is the electromagnetic torque, T_w is the torque due to the wind, J is the inertia of the rotor, D is the damping coefficient, $\omega_{rm} = \frac{\omega_r}{P}$ is the rotor mechanical speed, and P is the number of pole pairs of the generator.

The electromagnetic torque is described, for the *"Quadrature-Phase Commutator"* modelling [26], by the following expression:

$$T_e = -\frac{3}{2}PL_m(i_{sD}i_{rq} - i_{sQ}i_{rd}) \tag{8}$$

where regarding electromagnetic torque, one may observe that zero sequence currents i_{s0} and i_{r0} have not influence at all.

Finally, if we write (7) as a set of two ordinary differential equations, we get two mechanical state-variables for the wind generator:

$$\frac{d\theta_r}{dt} = \omega_r \tag{9}$$

$$\frac{d\omega_r}{dt} = \frac{1}{J}[P(T_e + T_w) - D\omega_r] \tag{10}$$

Consequently, the overall *electromechanical subtransient model of the wind generator* is described as a system of eight differential non-linear Eqs. (1)–(6), (9) and (10), in the state-space, being i_{sD}, i_{sQ}, i_{s0}, $i_{r\alpha}$, $i_{r\beta}$, i_{r0} electrical state-variables, and θ_r, ω_r mechanical state-variables.

3. Description of the wind farm

The wind farm chosen for its modelling has a radial shape, and is placed on "El Perdón" hill in Navarre, Spain. Diagram in Fig. 2 represents the outline of the overall system. This wind farm consists of $N = 40$ Squirrel Cage Induction Machine (SCIM) ABB G39-500 wind generators of 500 kW and a nominal voltage of 690 V, with 125 kVAR capacitive compensation. After a step-up Ynyn transformer of 690/20000 V, each induction machine is connected through subterranean lines with the common bus at 20 kV. There is another step-up Dyn transformer of 20/66 kV that connects the wind farm with a distribution line up to its connection through two Ynyn transformers of 68 MVA to the point of common coupling at 220 kV. The wind farm helps to feed two local loads at 66 kV, as sketched in the diagram.

Distribution line parameter values, loads and capacitor values have been provided by IBERDROLA S.A. utility. Loads connected to the distribution system are residential loads, so a dynamic model has not been considered of interest and they have been modelled as static.

To obtain the electrical parameters needed to define the dynamic model of the four-pole 500 kW Squirrel Cage Induction Machine, different tests were performed in a test bed placed in the origin factory. From those standard tests, parameter values collected in Table 1 were obtained.

When modelling the surrounding electrical elements, transformers are of great importance, particularly because of their vector group. In Spain, Yyn and Dyn connections are the most used in step-up transformers. The first one (Yyn) is straightforward to model, because there is not interaction between phases.

But Dyn connection presents additional difficulties when developing models of electrical networks, mainly due to the non diagonality of transformation matrices. As a consequence, these connections show coupling between phases and, to analyse the three-phase electrical network, it is not enough to keep into account just one per-phase equivalent circuit. A further complication is that the transformation matrices are singular, and this places conditions on the state-variables of the electrical network.

3.1. Wind data for the simulations

In order to attain realistic behaviours with the simulations of the wind farm, to have consistent wind data is a key issue. In all cases, wind simulation will be done using real time wind data recorded in a Spanish wind farm. A detail of the time progress of the wind speed on each generator, which was actually recorded in "Salajones" wind farm every one second, is shown in Fig. 3.

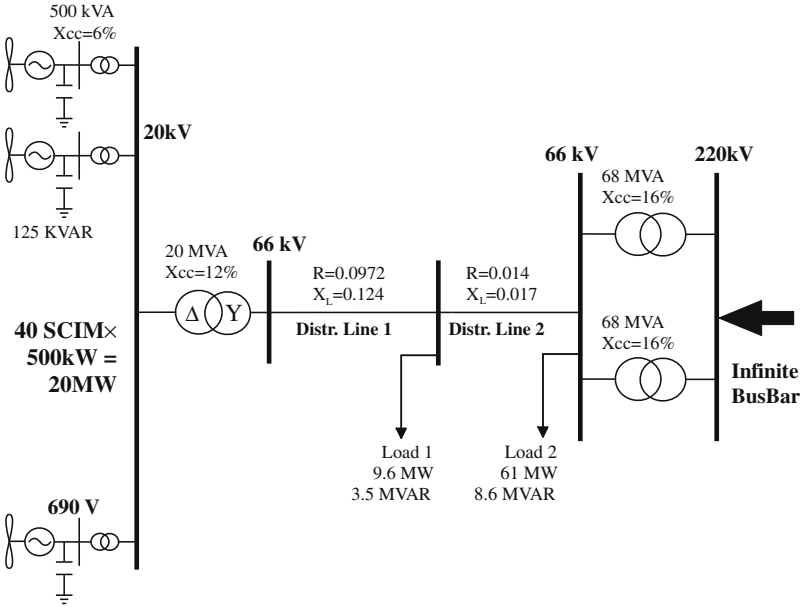

Fig. 2. Single-line diagram of "El Perdón" wind farm.

Table 1
Generator electric per-phase parameters.

Parameter	Value
R_s, stator resistance	5.1 mΩ
L_{ls}, stator leakage inductance	232.3 μH
L_s, stator inductance	13.2 mH
L_m, magnetizing inductance	31.9 mH
R_r, rotor resistance	101 mΩ
L_{lr}, rotor leakage inductance	2.38 mH
L_r, rotor inductance	82.1 mH
n, turns ratio	0.4
P, number of pole pairs	2

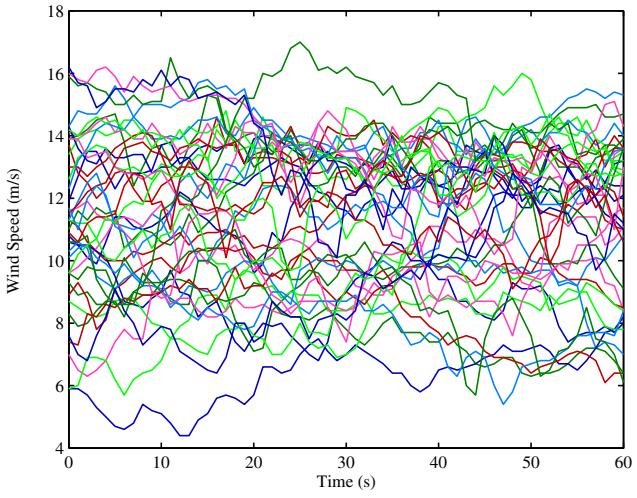

Fig. 3. Evolution of wind speed in each generator.

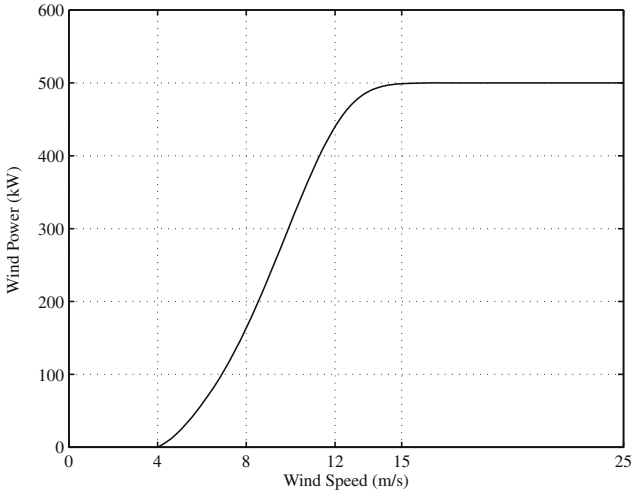

Fig. 4. Power generation curve of wind turbines of el "El Perdón" wind farm.

In addition, Fig. 4 shows the wind power generation curve of the wind turbines.

4. Integration of the surrounding electrical network in a compact matrix form

As stated previously, state equations of generators are given my means of (1)–(6), (9) and (10). But, in order to obtain the overall model of the wind farm, it is necessary to integrate the distribution network, with its loads and transformers in a compact form. Fig. 5 shows the per-phase equivalent circuit of "El Perdón" Wind Farm, where only one phase has been reflected.

4.1. Modelling objectives and state-variables

In Section 2 stator side variables of the generators are expressed in "$D-Q-0$" axes. However, it seems reasonable to express the surrounding network in "$a-b-c$" components, in order to keep the physical meaning of magnitudes. Consequently, it will be necessary, when needed, to perform either the Clarke's transformation from "$a-b-c$"—surrounding network—to the "$D-Q-0$" system—generators—, or the inverse Clarke's transformation from "$D-Q-0$" to three-phase quantities.

From state-space theory, it is well known that the number of states of a dynamical system equals the number of independent energy storage elements. The electrical network between the common busbar and the point of common coupling (Fig. 5) has five inductors, but their currents are not independent among them, because $i_2 = i_1 + i_{l1}$ and $i_{pcc} = i_2 + i_{l2}$. Thus, this electrical network has only three state-variables per-phase: i_{pcc}, i_1 and i_{l1}.

4.2. Development of the network model

4.2.1. Compensation capacitors

By effect of the compensation capacitors of each generator k ($k = 1, \ldots, N$), stator voltage is a state-variable of the network,

$$i_{suk} - i_{sk} = C\frac{dV_{sk}}{dt} \tag{11}$$

4.2.2. Subterranean lines

From each wind generator to the common busbar we can write,

$$V_{cb} = V_{sk} + \left(L_g^t + L_{su}\right)\frac{di_{suk}}{dt} + R_{su}i_{suk} \tag{12}$$

where L_g^t is the impedance of the step-up transformer of each generator, and R_{su}, L_{su} are the resistance and inductance of the subterranean lines.

The algebraic sum of N Eq. (12) formulated for each generator, as it is supposed that all generator transformers and subterranean lines are equal, produces

$$NV_{cb} = \sum_{k=1}^{N} V_{sk} + \left(L_g^t + L_{su}\right)\sum_{k=1}^{N}\frac{di_{suk}}{dt} + R_{su}\sum_{k=1}^{N} i_{suk} \tag{13}$$

If we now express $\bar{V}_s = \frac{1}{N}\sum_{k=1}^{N} V_{sk}$, and taking into account that $i_{cb} = \sum_{k=1}^{N} i_{suk}$, we can conclude that

$$V_{cb} = \bar{V}_s + \left(\frac{L_g^t}{N} + \frac{L_{su}}{N}\right)\frac{di_{cb}}{dt} + \frac{R_{su}}{N}i_{cb} \tag{14}$$

4.2.3. Distribution network

The equations of the distribution system that connects the wind farm to the main network are the following:

$$V_{pcc} = L_{pcc}^t\frac{di_{pcc}}{dt} + R_{l2}(i_{pcc} - i_1 - i_{l1}) + L_{l2}\frac{d}{dt}(i_{pcc} - i_1 - i_{l1}) \tag{15}$$

$$R_{l2}(i_{pcc} - i_1 - i_{l1}) + L_{l2}\frac{d}{dt}(i_{pcc} - i_1 - i_{l1}) = R_2(i_1 + i_{l1}) + L_2\frac{d}{dt}(i_1 + i_{l1}) + R_{l1}i_{l1} + L_{l1}\frac{di_{l1}}{dt} \tag{16}$$

$$R_{l1}i_{l1} + L_{l1}\frac{di_{l1}}{dt} = R_1 i_1 + \left(L_1 + L_{cb}^t\right)\frac{di_1}{dt} + V_{66} \tag{17}$$

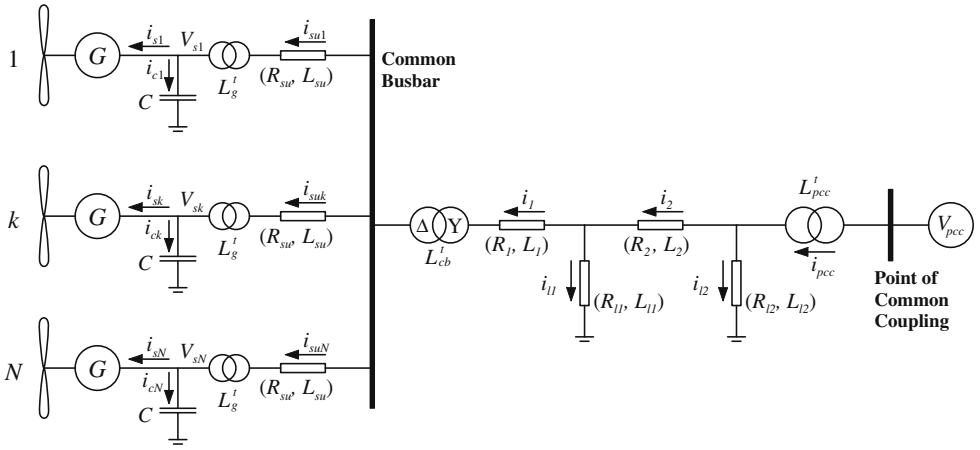

Fig. 5. Per-phase equivalent circuit of "El Perdón" wind farm.

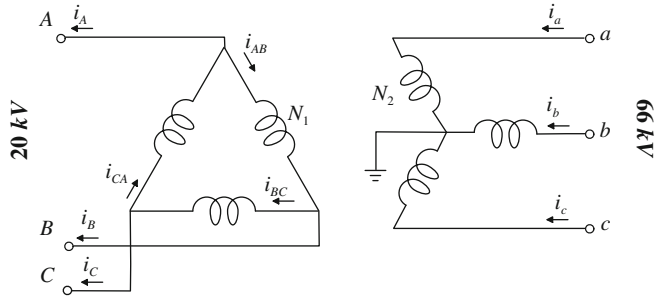

Fig. 6. Dyn transformer connection.

where V_{66} denotes voltage at the high side of the Dyn transformer.

4.2.4. Common busbar connection transformer

As already mentioned, the transformer which connects the common busbar of the wind farm (20 kV) with the distribution network (66 kV) has Dyn connection. Fig. 6 shows its internal configuration.

Consequently, the relation between voltages at low voltage and high voltage sides is

$$\begin{bmatrix} V_{66}^a \\ V_{66}^b \\ V_{66}^c \end{bmatrix} = \frac{1}{\sqrt{3}} \begin{bmatrix} 1 & -1 & 0 \\ 0 & 1 & -1 \\ -1 & 0 & 1 \end{bmatrix} \begin{bmatrix} V_{cb}^a \\ V_{cb}^b \\ V_{cb}^c \end{bmatrix}, \text{or } V_{66} = \frac{1}{\sqrt{3}} \mathrm{M_v} V_{cb} \tag{18}$$

In addition, the relation between currents of both sides of the transformer is

$$\begin{bmatrix} i_{cb}^a \\ i_{cb}^b \\ i_{cb}^c \end{bmatrix} = \frac{1}{\sqrt{3}} \begin{bmatrix} 1 & 0 & -1 \\ -1 & 1 & 0 \\ 0 & -1 & 1 \end{bmatrix} \begin{bmatrix} i_1^a \\ i_1^b \\ i_1^c \end{bmatrix}, \text{or } i_{cb} = \frac{1}{\sqrt{3}} \mathrm{M_i} i_1 \tag{19}$$

given that $i_{cb}^a = \sum_{k=1}^{N} i_{suk}^a$, $i_{cb}^b = \sum_{k=1}^{N} i_{suk}^b$, and $i_{cb}^c = \sum_{k=1}^{N} i_{suk}^c$.

If Eqs. (18) and (19) are replaced in (14), Eq. (17) takes the form

$$\begin{aligned} R_{l1} i_{l1} + L_{l1} \frac{\mathrm{d}i_{l1}}{\mathrm{d}t} &= R_1 i_1 + (L_1 + L_{cb}^t) \frac{\mathrm{d}i_1}{\mathrm{d}t} + \frac{1}{\sqrt{3}} \mathbf{M_V} \begin{bmatrix} \bar{V}_s^a \\ \bar{V}_s^b \\ \bar{V}_s^c \end{bmatrix} \\ &+ \frac{R_{su}}{3N} \mathbf{M_V M_i} \begin{bmatrix} i_1^a \\ i_1^b \\ i_1^c \end{bmatrix} + \frac{L_{su} + L_g^t}{3N} \mathbf{M_V M_i} \begin{bmatrix} \mathrm{d}i_1^a/\mathrm{d}t \\ \mathrm{d}i_1^b/\mathrm{d}t \\ \mathrm{d}i_1^c/\mathrm{d}t \end{bmatrix} \end{aligned} \tag{20}$$

4.2.5. State equations

Eqs. (15), (16) and (20) define the model of the surrounding network. They can be expressed as a system of nine linear equations, whose unknowns are the derivatives of the state-variables i_{pcc}, i_{l1}, i_1, for each of their components "$a-b-c$".

$$\mathbf{A} \cdot \begin{bmatrix} \mathrm{d}i_{pcc}^{abc}/\mathrm{d}t \\ \mathrm{d}i_{l1}^{abc}/\mathrm{d}t \\ \mathrm{d}i_1^{abc}/\mathrm{d}t \end{bmatrix} = \mathbf{b} \tag{21}$$

$$\mathbf{A} = \begin{bmatrix} (L_{pcc}^t + L_{l2})\mathbf{I} & -L_{l2}\mathbf{I} & -L_{l2}\mathbf{I} \\ L_{l2}\mathbf{I} & (-L_{l2} - L_2 - L_{l1})\mathbf{I} & (-L_{l2} - L_2)\mathbf{I} \\ \mathbf{0} & -L_{l1}\mathbf{I} & \begin{pmatrix} (L_1 + L_{cb}^t)\mathbf{I} + \\ + \frac{L_{su}+L_g^t}{3N} \mathbf{M_V M_i} \end{pmatrix} \end{bmatrix}$$

$$\mathbf{b} = \begin{bmatrix} V_{pcc}^{abc} - R_{l2}\left(i_{pcc}^{abc} - i_{l1}^{abc} - i_1^{abc}\right) \\ -R_{l2} i_{pcc}^{abc} + (R_{l1} + R_{l2} + R_2) i_{l1}^{abc} + (R_2 + R_{l2}) i_1^{abc} \\ R_{l1} i_{l1}^{abc} - \left(R_1 + \frac{R_{su}}{3N} \mathbf{M_V M_i}\right) i_1^{abc} - \frac{1}{\sqrt{3}} \mathbf{M_V} \bar{V}_s^{abc} \end{bmatrix}$$

where $(\cdot)^{abc}$ means a column vector with the "$a-b-c$" components of the variable under consideration, $\mathbf{I}$ is the 3×3 identity matrix, and $\mathbf{0}$ is the 3×3 zero matrix.

At this point, it is convenient to highlight that, given the parameters of the electrical network between the generators and the Point of Common Coupling, matrix of coefficients $\mathbf{A}$ of system (21) will be known, and it is possible to compute its inverse $\mathbf{A}^{-1}$ before the simulations. Consequently, in order to compute efficiently the state equations of i_{pcc}, i_{l1}, and i_1 at simulation stage, the equation to be followed is given next,

$$\begin{bmatrix} \mathrm{d}i_{pcc}^{abc}/\mathrm{d}t \\ \mathrm{d}i_{l1}^{abc}/\mathrm{d}t \\ \mathrm{d}i_1^{abc}/\mathrm{d}t \end{bmatrix} = \left(\mathbf{A}^{-1}\right) \cdot \mathbf{b} \tag{22}$$

with vector $\mathbf{b}$ to be computed, given V_{pcc}^{abc}, i_{pcc}^{abc}, i_{l1}^{abc}, i_1^{abc}, $\bar{V}_s^{abc}$, at every simulation step.

4.3. Additional remarks

In this section, state equation (22) of the electrical network surrounding the wind farm has been developed for the no-fault, no-islanding case. In order to obtain a more general model, it would be essential to incorporate i_{Fault}^{abc} as a state-variable of the model. As any electrical disturbance affects the system, the topology of

the network will change and, of course, $(\mathbf{A}^{-1})$ matrix will, as well. But the structure of the state equation, before, during and after the electrical disturbance will remain unchanged.

For the analysis of the behaviour of wind farms facing electrical disturbances, selection of i_{pcc}^{abc}, i_{Fault}^{abc} as state-variables is a must. When whichever electrical disturbance influences the system, the pre-fault and post-fault value of i_{Fault}^{abc} must be zero, and if there happens a loss of mains in any whatever phase, during this situation $i_{pcc} = 0$.

Simulation results of the behaviour of the wind farm under normal operation and electrical disturbances will be given below.

5. Aggregation of wind generators

Based on the electromechanical subtransient model of each generator—(1)–(6), (9) and (10)—and if capacitors, transformers and subterranean lines are included, for a wind farm of N wind turbines, dimension of the system increases linearly, with 14 differential equations per wind generator.

To face this dimension increase, a lot of modelling effort has been focused on a re-scaled equivalent generator model to simulate the wind farm. This model is usually called *Aggregated* or *Macro-generator*, as a parallelism with synchronous generators. Aggregation of constant speed wind generators is easily found in the literature [6–10,12]. However, this modelling approach merits closer examination, and its equations are described below.

5.1. Electrical model

The modelling objective is to obtain one aggregated model of the wind farm, such that there is some kind of equivalence between the original multi-machine model and the aggregated model, when seen from the common busbar of the wind farm.

The ideal aggregation could be stated as follows: under the same wind speed distribution and equal voltage at the common busbar, then identical output current from the wind farm. But in the multi-machine case, this current is the sum of the individual currents of the generators,

$$i_{cb} = \sum_{k=1}^{N} i_{suk} = \sum_{k=1}^{N} i_{sk} + \sum_{k=1}^{N} i_{Ck} \tag{23}$$

The *aggregated model of the wind farm* will be obtained as an unique fixed-speed generator whose stator side current is $\sum i_{sk}$, the current at the equivalent compensation capacitor is $\sum i_{Ck}$ and the current in the equivalent subterranean line is $\sum i_{suk}$.

The electric model of the induction machine in "$D-Q-0-d-q-0$" components [26] shows that the matrix equation of one fixed-speed induction machine can be expressed as

$$V_s = \mathbf{Z}_M \cdot i_s \tag{24}$$

with constant impedance matrix $\mathbf{Z}_M$. And, when the wind farm has N equal machines, the algebraic addition of their matrix equations is given next

$$\sum_{k=1}^{N} V_{sk} = \sum_{k=1}^{N} (\mathbf{Z}_M \cdot i_{sk}) = \mathbf{Z}_M \sum_{k=1}^{N} i_{sk} \tag{25}$$

If the sum of stator voltages is denoted as

$$\sum_{k=1}^{N} V_{sk} = N\bar{V}_s \tag{26}$$

then

$$\bar{V}_s = \left(\frac{\mathbf{Z}_M}{N}\right) \cdot \sum_{k=1}^{N} i_{sk} \tag{27}$$

With this definition, Eq. (27) has the same format as (24). As a result, it represents another induction machine—the equivalent or aggregated machine—whose *stator voltages must be interpreted as the average values, and currents as the sum* of the particular ones, and $\frac{\mathbf{Z}_M}{N}$ is the impedance matrix of this equivalent machine.

Therefore, in order to obtain the "$D-Q-0-d-q-0$" model of the aggregated generator, its electrical parameters should take the following values

$$R_s^N = \frac{R_s}{N}; \quad R_r^N = \frac{R_r}{N}; \quad L_s^N = \frac{L_s}{N}; \quad L_r^N = \frac{L_r}{N}; \quad L_m^N = \frac{L_m}{N} \tag{28}$$

In a similar way, based on the equation of the capacitor that improves the power factor of each induction machine

$$i_{Ck} = C\frac{dV_{sk}}{dt} \tag{29}$$

the equation of the equivalent capacitor is calculated by the algebraic addition of N equations. As all generators have the same capacitor value, and, applying the stator average voltage

$$\sum_{k=1}^{N} i_{Ck} = CN\frac{d\bar{V}_s}{dt} \tag{30}$$

then, the equivalent capacitor of the *N-machine* is N times the capacitor of each machine,

$$C^N = CN \tag{31}$$

Finally, Eq. (14) shows the relationship between average stator voltages, sum of subterranean line currents and voltage of the wind farm common busbar V_{cb}. As all generator transformers and subterranean lines are considered to be equal, the equivalent parameters of aggregated transformer and subterranean lines are

$$L_g^{tN} = \frac{L_g^t}{N}; \quad R_{su}^N = \frac{R_{su}}{N}; \quad L_{su}^N = \frac{L_{su}}{N} \tag{32}$$

5.2. Mechanical model

The mechanical model of the aggregated wind generator will be developed in a similar way to that of the electrical model. Based on Eq. (7) for a single machine, the mechanical equation of the wind farm will be the algebraic addition of N induction machines.

$$\sum_{k=1}^{N} T_{ek} + \sum_{k=1}^{N} T_{mk} = \sum_{k=1}^{N} J\frac{d\omega_{rmk}}{dt} + \sum_{k=1}^{N} D\omega_{rmk} \tag{33}$$

Due to several circumstances, such as different wind speeds, not all generators will have the same angular speed, but the average angular speed could be defined as

$$\bar{\omega}_{rm} = \frac{1}{N}\sum_{k=1}^{N} \omega_{rmk} \tag{34}$$

and the modified aggregate mechanical equation is

$$\sum_{k=1}^{N} T_{ek} + \sum_{k=1}^{N} T_{mk} = JN\frac{d\bar{\omega}_{rm}}{dt} + DN\bar{\omega}_{rm} \tag{35}$$

It looks as if the mechanical parameters of the macro-generator are the inertia and damping coefficients of a single one multiplied by the number of generators, and the mechanical speed of the macro-generator is the average value of those corresponding to the particular generators

$$J^N = JN; \quad D^N = DN; \quad \omega_{rm}^N = \bar{\omega}_{rm} \tag{36}$$

then, wind torque and electromagnetic torque of the aggregated machine will be, respectively, the algebraic addition of wind torques and electromagnetic torques of each machine, that is to say,

$$T_m^N = \sum_{k=1}^{N} T_{mk} \tag{37}$$

$$T_e^N = \sum_{k=1}^{N} T_{ek} \tag{38}$$

Expression (38) will be analysed in more detail. Based on the electromagnetic torque of the induction machine in "$D-Q-0-d-q-0$" components (Section 2)

$$T_e = -\frac{3}{2} P L_m (i_{sD} i_{rq} - i_{sQ} i_{rd}) \tag{39}$$

the algebraic addition for N machines should be

$$\sum_{k=1}^{N} T_{ek} = -\frac{3}{2} P L_m \sum_{k=1}^{N} \left(i_{sDk} i_{rqk} - i_{sQk} i_{rdk}\right) \tag{40}$$

On the other hand, if the equivalent electromagnetic torque is calculated from equivalent currents of the aggregated generator, its equation will be

$$T_e^N = -\frac{3}{2} P \frac{L_m}{N} \left(\sum_{k=1}^{N} i_{sDk} \sum_{k=1}^{N} i_{rqk} - \sum_{k=1}^{N} i_{sQk} \sum_{k=1}^{N} i_{rdk} \right) \tag{41}$$

Obviously, Eqs. (40) and (41) lead, in general, to different results, while expression (38) of the aggregated generator calls for their equality. This incongruity is the most serious drawback of macro-generator models.

On the other hand, it is observable that under adjoining rotor speeds among all generators, Eqs. (40) and (41) give similar results. This approximation is remarkable when the wind farm operates under normal conditions, with generator rotor slips close to or smaller than the nominal value (typically 1%).

The other side of the coin is, however, that under electrical disturbances and with different wind speeds for each generator, the aggregated model gives erroneous results. In spite of all criticisms about superfluous model complexity and computational time requirements, for transient stability studies there is no alternative, as it will be shown in the simulations.

6. Simulator implementation

As stated previously, Eqs. (1)–(6), (9) and (10) define the behaviour of the induction generators, and (22) the surrounding network. Based on these equations, the steps to implement the simulation algorithm are described below:

(1) Convert compensation capacitor voltages from three-phase V_s^{abc} to "$D-Q-0$" axes: v_{sD}, v_{sQ}, v_{s0}.
(2) Compute differential equations of the wind generators given by Eqs. (1)–(6), (9) and (10), in this case with $v_{rd}=0$, $v_{rq}=0$, $v_{r0}=0$ as the generators are Squirrel Cage.
   - *Multi-Machine case:* calculate $(8 \times N)$ derivatives of the state-variables: i_{sDk}, i_{sQk}, i_{s0k}, i_{rdk}, i_{rqk}, i_{r0k}, θ_{rk}, ω_{rk}, for each generator.
   - *Aggregated-Machine case:* calculate 8 derivatives of the state-variables: i_{sD}, i_{sQ}, i_{s0}, i_{rd}, i_{rq}, i_{r0}, θ_r, ω_r for the single macro-generator.
(3) Convert generator stator currents from "$D-Q-0$" axes to "$a-b-c$" values: i_s^{abc}.
(4) State equations of compensation capacitors (11) and calculate:
   - *Multi-Machine case:* $\bar{V}_s^{abc}$.
   - *Aggregated-Machine case:* V_s^{abc}.
(5) Using matrix equation of the surrounding network (22), calculate derivatives of i_1^{abc}, i_{l1}^{abc}, i_{pcc}^{abc}.
(6) Calculate V_{cb}^{abc} from Eq. (14), by considering that $i_{cb}^{abc} = \frac{1}{\sqrt{3}} \mathbf{M_i} i_1^{abc}$.
(7) Derivatives of subterranean line currents i_{suj}^{abc}, following (12).
(8) Integration of derivatives and go to the next simulation step (1).

This simulation algorithm shows that both models, multi-machine and aggregated-machine, share the same modelling structure. Evidently, the most significant difference between them comes from the number of state-variables. For "El Perdón" wind farm, with $N=40$ generators, in the case of the multi-machine model, the number of state-variables is $14 \times N + 9 = 569$; and for the aggregated model is 14 + 9 = 23.

The number of inputs (3 + N) is independent of the modelling approach and corresponds to voltage components at the point of common coupling with the transmission network V_{pcc}^{abc}, and the wind speed for each generator v_{wk}.

The number of outputs can be defined independently from the number of state-variables. It has been set to: stator current and voltage, mechanical speed of each generator, voltage and current at the wind farm busbar, currents of the different electrical loads of the network, and current at the connection point with the transmission network.

The simulation program developed to model the wind farm "El Perdón" has been implemented as a C-MEX S-Function for Simulink, with all parameters in the per-unit system—Base power: $S_B = 20$ MVA—. Using this simulation platform, several cases have been analysed in Sections 8 and 9. Simulation times will be shown for each case, taking a standard Pentium IV 3.2 GHz Personal Computer as simulation platform.

7. Alternative multi-machine model for validation purposes

In order to validate the results given by the simulations of the proposed multi-machine transient model, a simplified pseudo steady-state model has been developed. The modelling approach is the step-by-step formulation of the impedance matrix [**Z**] of the overall network [28], as used for the fault analysis in power systems. All distribution lines and transformers are modelled as complex impedances, and induction generators are described by conventional steady-state T-equivalent circuits [29].

As a consequence, this phasor-based modelling does not reflect any electrical transient phenomena. But, as T-equivalent circuits depend on the particular slip s of each generator, it is possible to simulate them—pseudo steady-state—in conjunction with their mechanical Eq. (10), where

$$T_e = \frac{3P}{\omega_s s} R_r' I_r'^2 \quad \omega_s = 2\pi f \quad f = 50 \text{ Hz} \tag{42}$$

The simulation algorithm for this simplified model is detailed next:

(1) Convert mechanical speeds to generator slips: $s_k = 1 - \frac{\omega_{rmk} P}{\omega_s}$.
(2) Compute impedance matrix [**Z**] of the overall network, following [28].
(3) Voltages at all nodes of the network are calculated as $V_{nodes} = \mathbf{Z} I_{nodes}$, where I_{nodes} except for the point of common coupling are all zero.
(4) Given the voltages at the inner node of the T-equivalent circuits of each generator (V_{rk}'), obtain $I_{rk}' = \frac{V_{rk}'}{R_r'/s_k + jX_{lr}'}$.
(5) Calculate T_{ek}, following (42).
(6) Compute differential equations of the wind generators given by (10).
(7) Integration of derivatives and go to the next simulation step (1).

8. Start-up of the wind farm

In this experiment, the objective is to simulate the start-up process of the whole wind farm. Initially, all the generators are stopped and they begin rotating freely impulsed by the power of the wind, until the rotor mechanical speed reaches synchronism and, in that moment, the generator is connected to the grid. Simulation lasting for 4 s wind farm time: Multi-machine: 24 s, aggregated model: 1.6 s.

Figs. 7 and 8 show, respectively, currents and voltages at the common busbar of the wind farm. For the multi-machine results, it is possible to detect the connection of each generator.

It should also be noted that, in the case of aggregated modelling, voltages and currents differ remarkably from multi-machine results. This is because, at connection time, with the aggregated model, the surrounding electrical network faces the sudden connection of a generator whose rated power is the total of the wind farm. And, for the multi-machine model, the connection of each generator happens when its particular speed is high enough.

In addition, Fig. 9 presents the behaviour of currents at the stator of the generators, computed with the multi-machine model. The instant of connection for each generator appears clearly.

Up to this point, Figs. 7–9 show RMS values of currents or voltages, computed from their instantaneous values. Obviously, this transient model allows the particular study of each variable of the overall network. Fig. 10 shows the behaviour of phase *a* instantaneous current at the startup of generator no. 32, whose connection happens at $t = 1.94$ s.

8.1. Validation of simulation results

First of all, this experiment has proved consistency among rated operation variables of the generators: When wind speed of the wind turbines takes its nominal value—$v_w = 16\ \frac{m}{s}$—, slip of the generators also reaches its rated value—1.8 %—, and so does the output stator current—447 A—.

In addition to that, Figs. 11–13 show, respectively, simulation results of mechanical speed, stator current and generated active power; for both multi-machine models: pseudo steady-state approach and full electromagnetic transient model.

Both simulation models present, under equivalent wind conditions, exactly the same connection times for each generator. And, in general, the pseudo steady-state model is able to forecast generator speeds and RMS values of electrical variables after their transient behaviour.

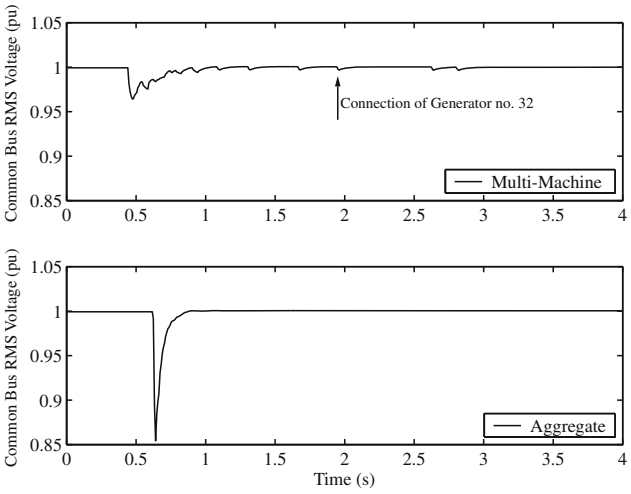

Fig. 8. Wind farm voltage at the common busbar.

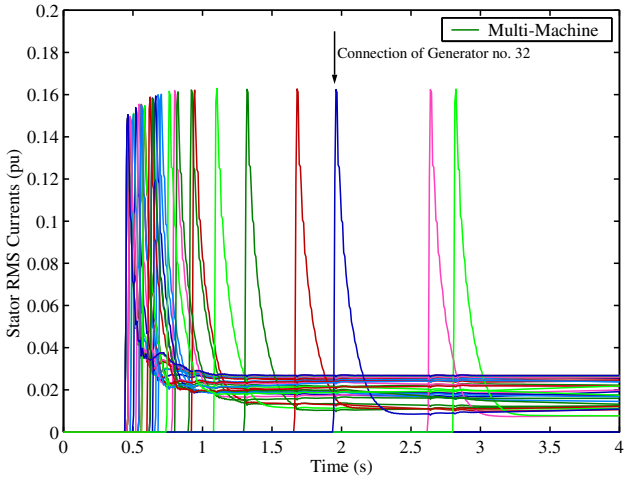

Fig. 9. Individual generator stator RMS current.

Obviously, pseudo steady-state simulation does not reflect all the interactions between the generators and the electrical network. In particular, the main issue when connecting generators is

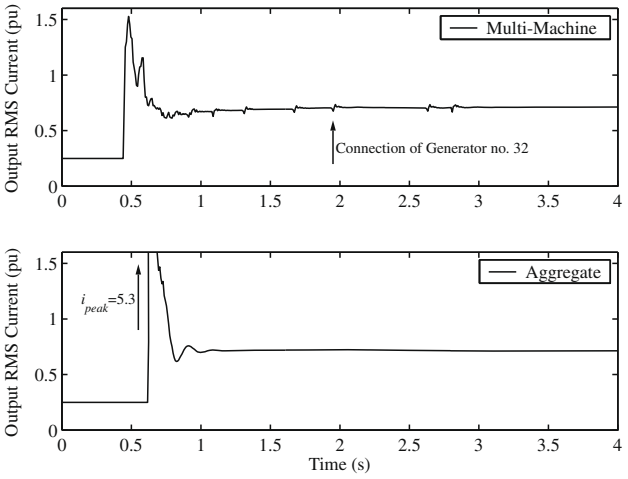

Fig. 7. Wind farm current measured at the common busbar.

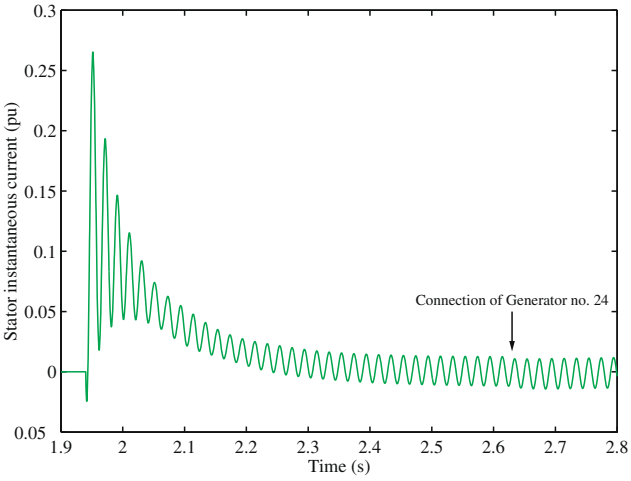

Fig. 10. Instantaneous current at connection of generator no. 32.

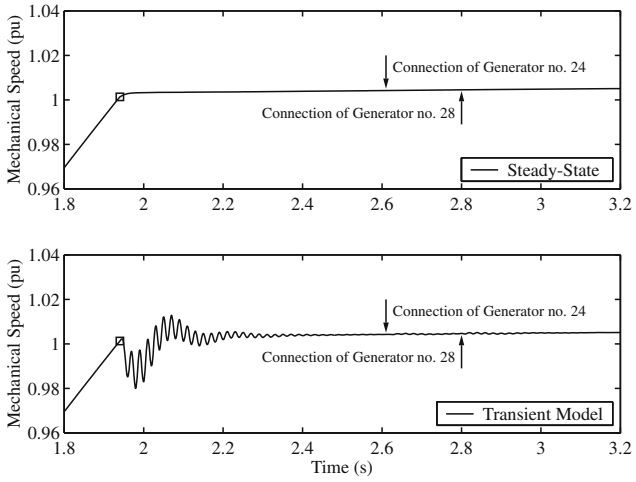

Fig. 11. Comparison of mechanical speeds at connection of generator no. 32.

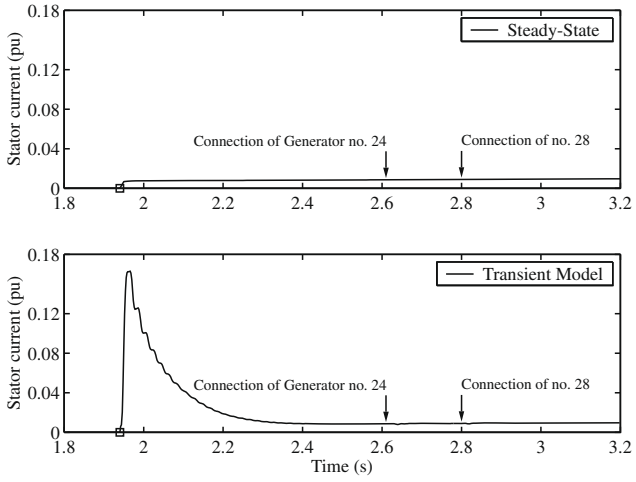

Fig. 12. Comparison of RMS stator currents at connection of generator no. 32.

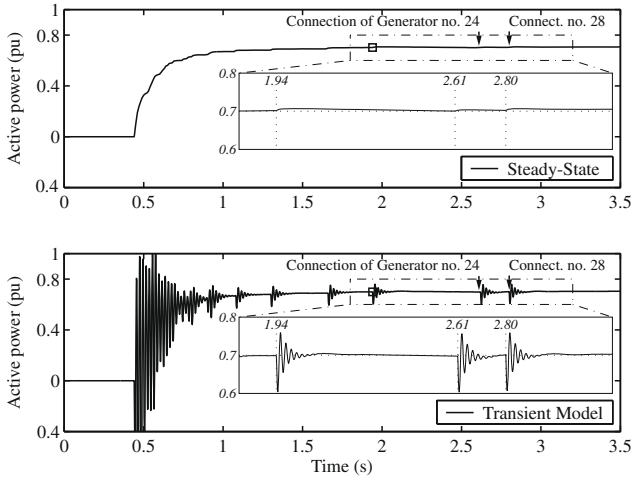

Fig. 13. Comparison of generated active power at startup of the wind farm.

the stator overcurrent needed to magnetize them. As connection happens when rotor speed reaches synchronism, for the pseudo steady-state case stator current is virtually zero, and it increases as the mechanical speed does, until an equilibrium is reached between T_w and T_e. But, simulation of the transient model shows clearly (Fig. 12) the magnetizing overcurrent—6× the rated one—.

Finally, Fig. 13 shows that the active power generated by the wind farm fluctuates, for each generator connection, much more than the $1/N$ ratio. This behaviour is clearly correlated with the mechanical speed (Fig. 11).

9. Islanding operation

The second test presents the behaviour of the wind farm when operating under islanding condition. In order to present more clearly simulation results, half of the generators will have a wind speed of 16 m/s, and the remaining half 8 m/s. The loss of mains begins at $t = 0.1$ s, and the reconnection is at $t = 0.7$ s. Simulation lasting for 2 s wind farm time: Multi-machine: 18 s, aggregated model: 0.8 s.

In this test, simulation results of the aggregated model, shown in Fig. 14, do not predict correctly the behavior of the wind farm. Whenever rotor speeds of all the generators are similar, the aggregated model really behaves with an average speed of all the generators. But, after reconnection, the aggregated model predicts erroneously a stable return to the previous condition, when actually half of the generators are not able to recover their previous mechanical speed.

Moreover, Fig. 15 shows the incongruity of the supposed addition torque for the aggregated model, compared with the real added up torque, as analysed in Eqs. (40) and (41). While there is no remarkable difference of rotor speeds among generators, the response of the aggregated model is very similar to that of the multi-machine model. But, after reclosing, its evolution is very different with respect to that of the multi-machine model.

9.1. Comparison of simulation results with steady-state ones

To start with, Fig. 16 presents similar evolutions of mechanical speeds of the generators, with half of them showing unstable behaviour, for both pseudo steady-state and transient models.

Regarding transient stability, pseudo steady-state simulation provides less conservative results. When loss of mains starts, mechanical speeds begin growing immediately. But, for the full transient model, there is an initial braking effect because of the fact that generators try to supply all the loads in the islanded network. This effect lasts as much as voltage at the common bus bar—shown in Fig. 17—does not collapse.

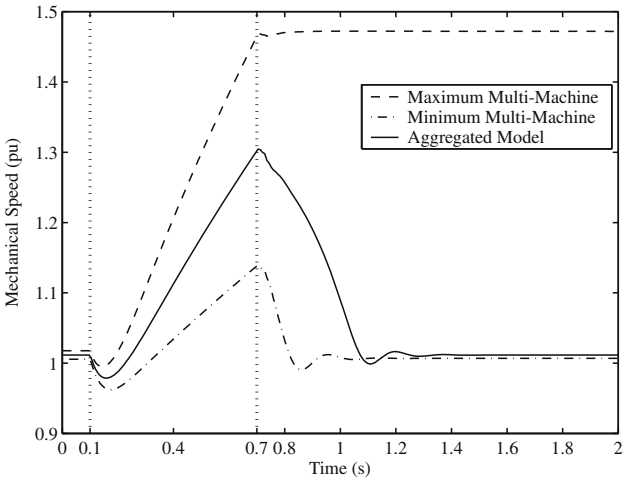

Fig. 14. Mechanical speed of the generators for the islanding test.

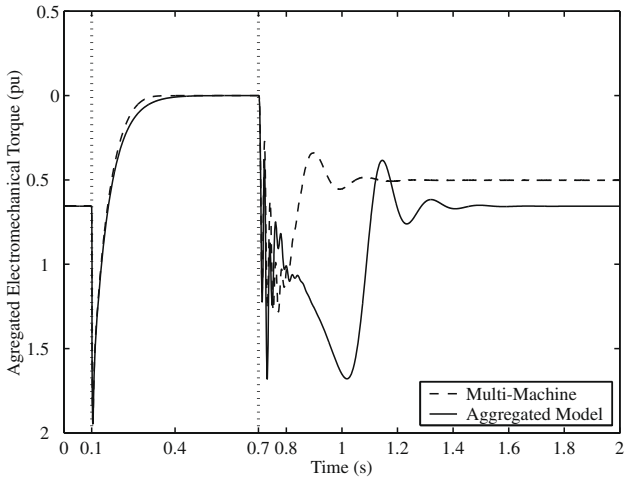

Fig. 15. Addition torque of all the generators for the islanding test.

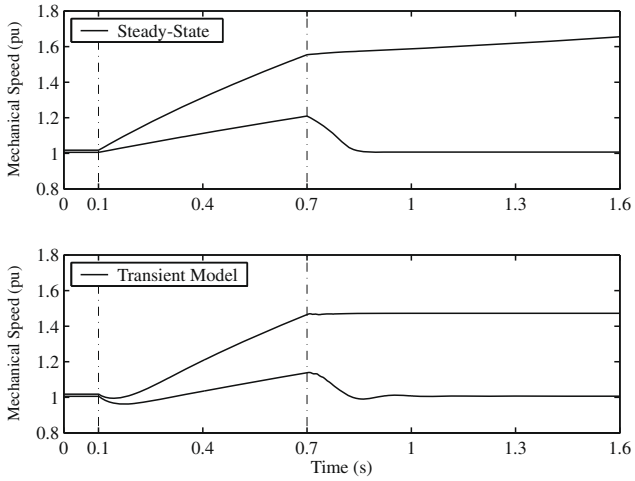

Fig. 16. Comparison of mechanical speeds when loss of mains occurs.

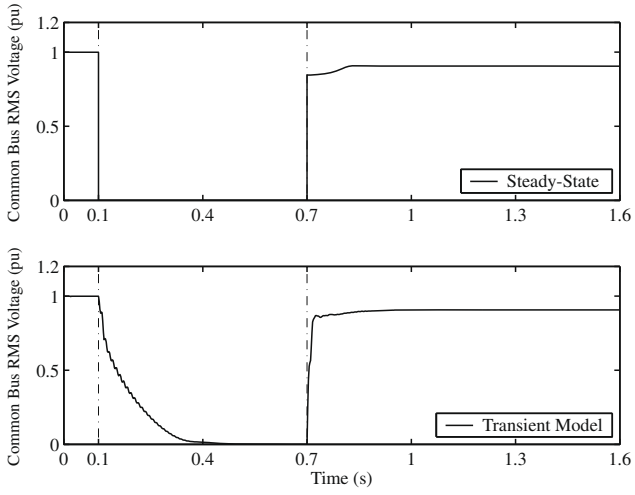

Fig. 17. Comparison of voltages at the common busbar when loss of mains occurs.

Both evolution alternatives, as for generator stability, are explained for the steady-state case as follows: when the wind farm is working under full islanding operation, the torque vs. speed

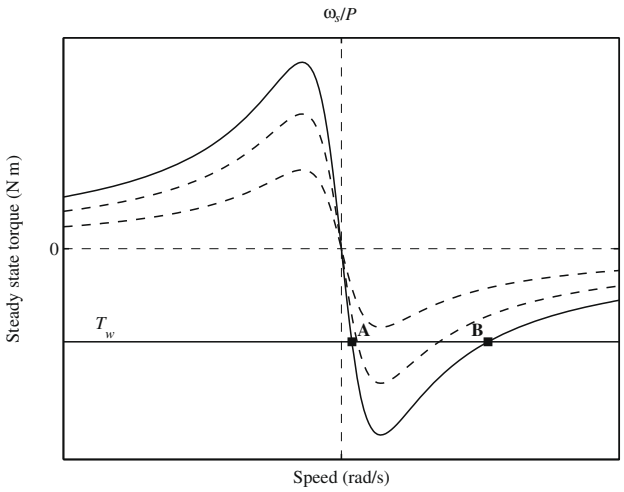

Fig. 18. Steady-state torque vs. speed of an induction generator.

characteristic of the generators cancels out totally. If, initially, the steady-state operating point of each of them is given in Fig. 18 by **A**, this is because the original electromagnetic torque equals the generating torque given by the wind. In other words, this is an initial equilibrium point.

When loss of mains occurs, the electromagnetic torque cancels out and, if the generating torque remains constant, an acceleration torque appears, which increases the rotor mechanical speed. When the wind farm is reconnected to the utility network, voltage at the common busbar trends toward its pre-fault value. If, due to the duration of the loss of mains, the rotor mechanical speed exceeds that of point **B**, an acceleration torque will appear again. In this situation, such generators will not be able to regain its previous operating point **A**.

10. Conclusion

Wind generators have been modelled in terms of the *Quadrature-Phase Commutator* full transient model, with six electrical state-variables, and two more mechanical. The electrical network from the wind farm common busbar up to the point of common coupling has also been modelled in state-space. Delta-wye connection of the transformer at the wind farm common busbar has also been integrated in the overall model, and rated values of the generators have also been verified.

The approximation of *aggregated* modelling of Squirrel Cage Induction Machines has been discussed in detail, providing the physical meaning of aggregated parameters and variables. The aggregated induction generator works in an average operating point corresponding to average rotor speeds and average stator voltages. But this modelling approach is only valid when all the generators have similar angular speeds. Generalization of this modelling could mask the real evolution of each wind generator that might be very different to the evolution of the re-scaled machine.

Steps needed for the simulation of the overall system have been specified. The multi-machine model and the aggregated approximation share the same simulation structure. As a consequence, it is quite straightforward to simulate both models in the same platform.

An alternative simplified multi-machine model for validation of the proposed full transient model has been developed. This model is based on the formulation of the impedance matrix of the overall network, as used for the fault analysis problem. The model is simulated according to the particular slip of each generator. Compari-

son between results of the full transient model and those of the simplified one shows that, in general, both models predict the same pseudo steady-state behaviours.

The proposed modelling method has been found appropriate for the analysis of different disturbances affecting the wind farm. Simulation results show that aggregated models are not able, in general, to predict correctly the real behaviour of the wind farm.

The methodology has been applied to the real wind farm of "El Perdón". Its model has been implemented as a C-MEX S-function for Simulink. With those compiled models, simulation speeds are clearly superior to that of block-based models.

The multi-machine model not only describes more precisely the behaviour of the wind farm, but it is also indispensable for the design and validation of new operational strategies for wind farms. This model is a necessary tool for challenging problems such as active and reactive power control.

Acknowledgements

We would specially like to thank J. Molina and V. Moreno for their helpful comments. The authors are also grateful to the induction generator manufacturing company, INDAR, and specially to J. Garde, for their contribution in providing the electric machine characteristics. We would also like to thank M. Irizar and J. L. Berasategui from the Spanish utility IBERDROLA. This work has been carried out in the research group GIU07/45 of the University of the Basque Country (UPV/EHU) and has been supported by the research project DPI2006-06612 of the Ministerio de Educacion y Ciencia (Spain).

References

[1] EWEA. European capacity map 2007, 2008, <http://www.ewea.org>.
[2] Heier S. Grid integration of wind energy conversion systems. New York: John Wiley & Sons; 1998.
[3] Eltra. Technical regulation for the properties and the regulation of wind turbines. Tech. rep., Eltransmission.dk A/S, Fredericia, Denmark, December 2004.
[4] Grid code, high and extra high voltage. Tech. rep., E.ON Netz GmbH, Bayreuth, Germany, August 2003.
[5] The grid code. Tech. rep., National Grid Electricity Transmission plc, London, UK, May 2006.
[6] Muljadi E, Wan Y, Butterfield CP, Parsons B. A study of a wind farm power system. Tech. rep., NREL/CP-500-30814, National Grid Electricity Transmission plc, London, UK, Janauary 2002.
[7] Slootweg JG, Kling WL. Modelling wind turbines for power system dynamics simulations: an overview. Wind Eng 2004;28(1):7–26.
[8] Akhmatov V. Analysis of dynamic behaviour of electric power systems with large amount of wind power. PhD thesis, Electric Power Engineering, Ørsted-DTU, Technical University of Denmark, Lyngby, Denmark, 2003.
[9] Slootweg JG. Wind Power Modelling and Impact on Power System Dynamics. PhD thesis, Ridderprint Offsetdrukkerij B.V., Ridderkerk, the Netherlands, 2003.
[10] Kazachkov YA, Feltes JW, Zavadil R. Modeling wind farms for power system stability studies. In: 2003 IEEE power engineering society general meeting (IEEE cat. no. 03CH37491), Toronto, Canada, 2003. p. 1526–33.
[11] Rodríguez JM, Fernández JL, Beato D, Iturbe R, Usaola J, Ledesma P, et al. Incidence on power system dynamics of high penetration of fixed speed and doubly fed wind energy systems: study of the spanish case. IEEE Trans Power Syst 2002;17(4):1089–95.
[12] Ledesma P, Usaola J, Rodríguez JL. Transient stability of a fixed speed wind farm. Renew Energy 2003;28:1341–55.
[13] Zubia I, Ostolaza X, Molina J. Analysis of transient stability of fixed speed wind farms. In: 16th International conference on electrical machines ICEM2004, Cracow, Poland, 2004. p. 1–8.
[14] Akhmatov V, Knudsen H, Nielsen AN, Pedersen JK, Poulsen NK. Modelling and transient stability of large wind farms. Elec Power Energy Syst 2003;25:123–44.
[15] Ledesma P, Usaola J. Minimum voltage protections in variable speed wind farms. In: IEEE porto power tech conference, Porto, Portugal, 2001. p. 1–6.
[16] Tapia A, Tapia G, Ostolaza JX, Sáenz JR. Modeling and control of a wind turbine driven doubly fed induction generator. IEEE Trans Energy Convers 2003;12(2):194–204.
[17] Tapia G, Tapia A, Ostolaza JX. Proportional-integral regulator-based approach to wind farm reactive power regulation for secondary voltage control. IEEE Trans Energy Convers 2007;22(2):488–98.
[18] Camblong H, de Alegria IM, Rodriguez M, Abad G. Experimental evaluation of wind turbines maximum power point tracking controllers. Energy Convers Manage 2006;47:2846–58.
[19] Zubia I. Analysis and design of operation strategies for the running of wind farms. PhD thesis, in Spanish, Servicio editorial de la Universidad del País Vasco, Bilbao, Spain, 2004.
[20] Zhang J, D'ysko A, O'Reilly J, Leithead WE. Modelling and performance of fixed-speed induction generators in power system oscillation stability studies. Elec Power Syst Res 2008:1–9. doi:10.1016/j.epsr.2008.01.003.
[21] García-Gracia M, Comech MP, Sallán J, Llombart A. Modelling wind farms for grid disturbance studies. Renew Energy 2008:1–13. doi:10.1016/j.renene.2007.12.007.
[22] Muljadi E, Parsons B. Comparing single and multiple turbine representations in a wind farm simulation. In: European wind energy conference, Athens, Greece, 2006. p. 1–10.
[23] Qiao W, Harley RG, Venayagamoorthy GK. Dynamic modeling of wind farms with fixed-speed wind turbine generators. In: IEEE power engineering society general meeting, Tampa, Florida, 2007. p. 1–8, doi: 10.1109/PES.2007.386283.
[24] Stavrakakis GS, Kariniotakis GN. A general simulation algorithm for the accurate assessment of isolated diesel-wind turbines systems interaction. Part i:a general multimachine power system model. IEEE Trans Energy Convers 1995;10(3):577–83.
[25] Stavrakakis GS, Kariniotakis GN. A general simulation algorithm for the accurate assessment of isolated diesel-wind turbines systems interaction. Part ii: implementation of the algorithm and case-studies with induction generators. IEEE Trans Energy Convers 1995;10(3):584–90.
[26] Vas P. Vector control of AC machines. New York: Oxford University Press; 1990.
[27] Vas P. Sensorless vector and direct torque control. New York: Oxford University Press; 1998.
[28] Gross CA. Power system analysis. New York: John Wiley & Sons; 1986.
[29] Vas P. Electrical machines and drives: a space-vector theory approach. New York: Oxford University Press; 1992.